Atmospheric Environment 316 (2024) 120169

Contents lists available at ScienceDirect

Atmospheric Environment

journal homepage: www.elsevier.com/locate/atmosenv

Online monitoring of carbonaceous aerosols in a northern Chinese city: Temporal variations, main drivers, and health risks

Xiansheng Liu [a], Xun Zhang [b], Bowen Jin [b], Hadiatullah Hadiatullah [c], Luyao Zhang [d], Pei Zhang [e], Tao Wang [f,*], Qihong Deng [g], Xavier Querol [a]

[a] Institute of Environmental Assessment and Water Research (IDAEA-CSIC), Barcelona, Spain
[b] Beijing Key Laboratory of Big Data Technology for Food Safety, School of Computer Science and Engineering, Beijing Technology and Business University, Beijing, China
[c] School of Pharmaceutical Science and Technology, Tianjin University, Tianjin, China
[d] Department of Earth System Science, Ministry of Education Key Laboratory for Earth System Modeling, Institute for Global Change Studies, Tsinghua University, Beijing, 100084, China
[e] School of Environment, Nanjing Normal University, Nanjing, 210023, China
[f] Shanghai Key Laboratory of Atmospheric Particle Pollution and Prevention, Department of Environmental Science & Engineering, Fudan University, Shanghai, 200433, China
[g] School of Public Health, Zhengzhou University, Zhengzhou, 450001, Henan, China

HIGHLIGHTS

- Online sampling of carbonaceous aerosols (CAs) was firstly assessed in Yanzhou.
- The weight of SOC in OC was highest in summer (60%) and lowest in winter (26%).
- HPBL, AT, RH, and AP are the driving factors for different CAs.
- Increased eBC caused relatively high health risk to children.

GRAPHICAL ABSTRACT

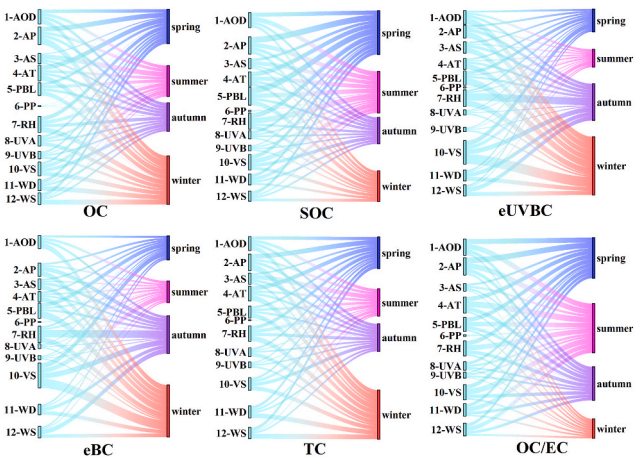

ARTICLE INFO

Keywords:
Carbonaceous aerosols
Organic carbon
Black carbon
Health risk

ABSTRACT

This study examined the variability and source of carbonaceous aerosols, encompassing total carbon (TC), organic carbon (OC), and secondary organic carbon (SOC) for the years 2019–2020, as well as equivalent black carbon (eBC) and equivalent ultraviolet BC (eUVBC) data spanning 2019–2022, in the context of a typical northern Chinese city: Yanzhou. Averaged concentrations of TC, OC, SOC, eBC, eUVBC, and the ratio (OC/elemental carbon (EC)) reached 11.1 ± 6.7, 8.9 ± 5.1, 3.9 ± 2.0, 3.1 ± 1.3, and 4.3 ± 2.4 μg/m^3, and 5.0 ± 2.2,

* Corresponding author.
E-mail address: wangtao_fd@fudan.edu.cn (T. Wang).

https://doi.org/10.1016/j.atmosenv.2023.120169
Received 5 July 2023; Received in revised form 1 October 2023; Accepted 29 October 2023
Available online 31 October 2023

respectively. The concentrations of TC, OC, eBC, and eUVBC were higher in winter, followed by spring and autumn, and summer, while SOC presented the opposite seasonal patterns. The diurnal variations of TC, OC, eBC, and eUVBC exhibited a bimodal pattern with peaks in the early morning (08:00–09:00 LT) and late evening (00:00–01:00 LT) and a trough in the afternoon (14:00–16:00 LT), pointing to vehicular emission and meteorological dispersion as major drivers of the hourly variability. The results obtained from the EC tracer method and minimum R squared (MRS) revealed that r(SOC/OC) were highest in summer (60%) and lowest in winter (26%), showing a fast summer photochemical oxidation of volatile organic compounds (VOCs) that generate SOC. In this study, the influence of meteorological conditions on the weighting of diverse carbonaceous aerosols was quantified using a machine learning method. Results showed that the main drivers of carbonaceous aerosols were height of the planetary boundary layer (HPBL), ambient temperature (AT), relative humidity (RH), and atmospheric pressure (AP) in all seasons. Additionally, the potential health risks of eBC based on the equivalent passive smoking of cigarettes (PSC) suggested that there was a certain level of human health risk in this city. The obtained results will provide more in-depth and comprehensive understanding of carbonaceous aerosol pollution and management strategies.

1. Introduction

The atmospheric aerosol is made of a complex mixture of solid and liquid particles suspended in the air, which can be classified into six categories: sulfate, nitrate, ammonium, carbonaceous components, dust, sea-salt, and mine (Chen et al., 2020; Colbeck and Lazaridis, 2010; Pöschl, 2005). Of these, carbonaceous aerosols make up a significant portion of the overall concentration of fine-mode particulate matter (PM) in the atmosphere, up to 50% in urban areas of China (H. Zhang et al., 2019), and even higher proportions in Europe and US (Jimenez et al., 2009; In'T Veld et al., 2021). These might affect human health environmental quality, global climate, and atmospheric visibility, thus causing worldwide concerns (Bond et al., 2013; Li et al., 2021; Liu et al., 2022). These aerosols have an airborne lifespan of up to few weeks, which accounts for their frequent atmospheric long-range transport, potentially impacting global air quality and further influencing the global climate (Dumka et al., 2019).

The carbonaceous aerosols in the atmosphere comprise carbonate (mineral) carbon (CC), organic carbon (OC) and elemental carbon (EC), and the later class is also known as black carbon (BC) (Chen et al., 2023) or equivalent BC (eBC, (Petzold et al., 2013). OC typically encompasses primary and secondary organic compounds, such as hydrocarbons and carboxylic acids (Alves et al., 2012; Duan et al., 2005), which belong to hazardous species (Wu and Yu, 2016; Xu et al., 2015). Fine aerosol mode constitutes a substantial mass portion of carbonaceous aerosols (Gilardoni et al., 2011). In addition, OC compounds have a strong absorption capacity for Ultraviolet (UV) and Infrared (IR) radiation (Laskin et al., 2015). This may be operationally defined as UV absorbing BC (UVBC), brown carbon (BrC), or absorbing OC (Esposito, 2012). In general, measurement of UV absorbing BC at 370 nm is defined as equivalent UVBC (eUVBC) and measurement of BC at 880 nm is defined as equivalent BC (eBC) (Peng et al., 2018).

eBC is a primary and important component of atmospheric aerosols and derived from the incomplete combustion of fossil fuels, biomass, wastes, and forest fires (Hopkins et al., 2007; Long et al., 2013). There is a body of evidence indicating the adverse health effects of eBC, although it seems that it is not eBC, per se, which might cause these effects, but specific organic pollutants enriched in high eBC particles (Janssen et al., 2012; Verma et al., 2022). Therefore, eBC may act as a carrier of a wide range of chemicals with different toxicities into the lungs. Since early 2012, the International Agency for Research on Cancer (IARC) classified diesel soot, which was usually used synonymously with eBC (but the first term also includes the organic species co-emitted with eBC), as carcinogenic to humans (Group 1) (IARC, 2012). eBC can be measured by using light absorption procedures (Petzold et al., 2013). The absorption units are converted into atmospheric concentrations by using a mass absorption cross-section (MAC) that has been obtained by comparing the absorption measurements with the analysis of EC. That's why the term eBC is usually applied.

In previous studies, carbonaceous aerosols were typically monitored using offline methods (Glasius et al., 2018; Xie et al., 2019; Zhao et al., 2013). However, offline sampling, may fail to achieve high resolution data, therefore causing a significant priority gap in the observed data and hindering the accurate reproduction of the pollution characteristics of carbonaceous aerosols in the real atmosphere (Srivastava and Naja, 2021). Recently, an increasing number of studies (Liu et al., 2022; Rigler et al., 2020; Savadkoohi et al., 2023; Srivastava et al., 2019; Yao et al., 2020; Yus-Díez et al., 2022) selected online sampling due to the generation of extensive data sets with fine granularity even during short periods of pollution. This approach offers two significant advantages. Firstly, the enhanced temporal resolution allows for a more thorough analysis and comprehension of the temporal patterns exhibited by distinct carbonaceous aerosols, thereby providing a more detailed examination and comparison of their pollution attributes and potential sources (Savadkoohi et al., 2023; Trechera et al., 2023). Secondly, the increased volume of data presents an opportunity for machine learning, enabling the quantitative elucidation of the non-linear relationship between different types of carbonaceous fractions and their influencing factors (Dai et al., 2023).

Given the substantial seasonal variations of carbonaceous aerosol concentrations, it is crucial to delve deeper into understanding the relationships between OC and BC aerosols across different seasons, and to identify the primary atmospheric drivers. Therefore, continuous online monitoring of diverse carbonaceous components is essential, allowing for the constant surveillance of environmental parameters. This immediate feedback is crucial for identifying short-term fluctuations and rapid changes in pollutant levels. Yanzhou is located in the north of China and situated in Shandong Province, inland from the coast (Fig. S1). The city has a population close to 0.54 million. The study area has a temperate monsoon climate with low wind speed and high humidity, which is typical of cities in the northern region of China. Although there have been investigations into the levels of near-surface carbonaceous aerosols in northern Chinese cities (Cao et al., 2007; Dong et al., 2022; Q. Liu et al., 2018), no associated information is available for Yanzhou and there also remains a notable gap in systematic studies concerning online carbonaceous aerosols about temporal variations, main drivers, and health risks.

This study, for the first time, studied the diverse carbonaceous particles in Yanzhou, including the concurrent high-time-resolution measurements of total carbon (TC) and OC during 2019–2020 and eUVBC and eBC during 2019–2022. The main objectives of this study are to investigate of the variability of carbonaceous aerosols and their formation drivers in Yanzhou, briefly, (1) determining ambient TC, OC, SOC, eUVBC, and eBC concentrations and comparing Yanzhou with other cities worldwide; (2) assessing their seasonal and diurnal variations and identifying their major sources; (3) assessing the carbonaceous aerosols phenomenology and their major drivers by machine learning analysis, and (4) estimating potential health risks of eBC exposure.

2. Material and methods

2.1. Measurements

Measurements of hourly carbonaceous aerosols (TC, OC, eUVBC, and eBC) and the corresponding auxiliary data, including meteorological data (atmospheric stability (AS), atmospheric pressure (AP), ambient temperature (AT), relative humidity (RH), wind direction (WD), wind speed (WS), precipitation (PP), height of the planetary boundary layer (HPBL),aerosol optical depth (AOD), and visibility (VS), were carried out at the Automatic Air Quality Monitoring Superstation in Yanzhou (35.43° N, 116.6° E) from August 1, 2019 to December 31, 2022. The sampling height of ~20 m above ground levels accurately reflects the air quality of Yanzhou city. The instruments were checked and maintained each week, and calibrated every two weeks. All data used in this study were recorded in Beijing Time (China Standard Time, UTC+8).

In this study, AS, AP, AT, RH, WD, WS, PP, and HPBL are used as the drivers of carbonaceous aerosols for their direct or indirect influences on the concentration data, while AOD and VS are used as tracers due to the feedbacks they received from the carbonaceous aerosol loadings.

2.2. Set-up and instrumentation

Ambient concentrations of TC, OC, and EC were determined by means of an online thermo-optical-transmission (TOT) analyzer (Sunset Model 4/OCEC (RT-4), USA), with a $PM_{2.5}$ impactor inlet. TC was determined as OC + EC. In emissions inventories and climate science, EC is usually synonymous of eBC (Cheng et al., 2011). In this study, EC is used for the TOT data (Hopke et al., 2006), while eBC was used to describe and interpret data from optical measurements.

Concentrations of BC were measured by an Aethalometer (Magee Scientific, Model AE33, Slovenia). This instrument measures and records the light attenuation by PM (continuously deposited on a Teflon-coated glass fiber filter tape) at seven wavelengths (370 nm, 470 nm, 520 nm, 660 nm, 880 nm, and 950 nm), ranging from UV to IR, with a temporal resolution of 1 min and a sampling flow rate of 5.0 l/min. The measured attenuation at 880 nm is interpreted as BC, which is the primary absorber of visible light. It is generated through the incomplete combustion of materials containing carbon (Olson et al., 2015). The measurement at 370 nm, interpreted as equivalent UVBC (eUVBC), signifies light-absorbing particulate matter emitted from smoldering organic materials (Sandradewi et al., 2008).

The BC concentrations were converted into eBC ones by using a MAC obtained locally with the co-located EC TOT measurements and the absorption measurements, the MAC supplied by the aethalometer's manufacturers might differ considerably from the ones obtained with collocated EC measurements. Therefore, since eBC and EC represent the same carbonaceous aerosol, the eBC concentrations was used for the random forest regression of the eBC time-series and meteorological factors or atmospheric parameters.

Furthermore, AS, AP, AT, RH, WD, WS, and PP data were recorded, with 1 min integration time, by the weather station system WMR300 (Oregon Scientific, USA). AOD, HPBL and VS were monitored using aerosol lidar (SM-200, Zhongke Guangbo Quantum Technology Co., LTD).

2.3. Estimation of secondary organic carbon

A fraction of OC that originated from VOC precursors by photo-oxidation and aqueous-phase reaction processes is defined SOC. Its concentration at Yanzhou was estimated here based on an EC-tracer method (Castro et al., 1999; Q. Zhang et al., 2019).

$$SOC = OC - [OC/EC]_{pri} \times EC \quad \text{(Eq.1)}$$

The Minimum R squared (MRS) method was used to select $(OC/EC)_{pri}$ following (Wu and Yu, 2016). In this study, the MRS of spring, summer, autumn, and winter is 3.04, 2.08, 1.94, and 2.88, respectively (Fig. S2).

2.4. Assessment of the health risk of eBC exposure

In this study, the health risks of passive smoking, environmental tobacco smoke (ETS), were estimated to be equal to the health risk of eBC due to their similar characteristics (Ali et al., 2021; Pani et al., 2020; van der Zee et al., 2016). For example, (i) both have similar health effects, (ii) both are mostly unavoidable and involuntary, and (iii) both have similar exposure routes, i.e., inhalation (van der Zee et al., 2016). Therefore, this approach has been applied to assess the health risks of eBC using the equivalent numbers of passively smoked cigarettes (NPSC) (van der Zee et al., 2016) to establish health risk estimates. Briefly, four health endpoints, including low birth weight (LBW) implying a birth weight <2.5 kg after 37-week gestation, percentage lung function decrement of school aged children (PLFD), lung cancer (LC), and cardiovascular mortality (CM) for adults, were selected to evaluate the health risks (van der Zee et al., 2016). The equivalent N_{PSC} can be calculated as follows:

$$N_{psc} = \frac{\beta_{eBC}}{\beta_{cigartte}} \times \Delta C = \frac{\frac{ln\ (RR_{eBC})}{\Delta concentration}}{\frac{ln\ (RR_{EST})}{N_a}} \times \Delta C \quad \text{(Eq.2)}$$

where:

$$\beta_{eBC} = \frac{ln\ (RR_{eBC})}{\Delta concentration} \quad \text{(Eq.3)}$$

is the regression coefficient per 1 μg/m^3 for eBC;

$$\beta_{cigartte} = \frac{ln\ (RR_{EST})}{N_a} \quad \text{(Eq.4)}$$

is the regression coefficient per cigarette; Δconcentration = 1 μg/m^3 for eBC;

where, ΔC refers to the difference between the monitored and background concentrations of eBC (the background eBC level was determined at the urban background site of was chosen as 0.272 μg/m^3 (data from Waliguan Observatory based on (Ma et al., 2003). RR_{eBC} is the relative risk for the association between eBC and the health endpoint; RR_{ETS} is the relative risk for ETS exposure; and N_a represents the assumed number of cigarettes, which is 9 for children exposed to parental smoking in relation to the risk of PLFD and 7 for adults in relation to the risk of LBW for infants of non-smoking mothers, CM, and LC (van der Zee et al., 2016).

2.5. Statistical analysis

Due to the missing data of OC and EC during 2021 and 2022, the data obtained between 2019 and 2020 were used to analyze the temporal variations of OC, SOC, TC, and OC/EC, while the whole dataset were used for the discussion on eBC and eUVBC. The data here are reported in the form of averaged concentration ± standard deviation. The correlations between hourly meteorological and atmospheric factors were analyzed by evaluating the 'R' of Pearson correlation coefficient, for each season. The analysis of significant differences of carbonaceous aerosols, meteorological factors, and health risks posed by eBC aerosol was carried out by one-way Analysis of Variance (ANOVA) employing Duncan's Multiple Range Test at $p < 0.05$ and $p < 0.01$, using SPSS Software (IBM SPSS Statistics 25, Chicago, IL, USA). In addition, it is worth noting that, some meteorological indicators, serving as drivers, might be significantly correlated with carbonaceous aerosols via non-linear relationships. Random forest can solve this nonlinear relationship well (Brokamp et al., 2017). Hence, the multivariate relationships between carbonaceous aerosols and the meteorological drivers (AS, AP,

Table 1
Average and standard deviation (μg/m^3) concentrations of TC, OC, SOC, eBC, and eUVBC measured in Yanzhou with other cities worldwide (TC, OC, and SOC monitored during 2019–2020, and eBC and eUVBC monitored during 2019–2022).

Time	Site	TC	OC	SOC	eBC	eUVBC	Reference
Annual	Yanzhou	11.1 ± 6.7	8.9 ± 5.1	3.9 ± 2.0	3.1 ± 1.3	4.3 ± 2.2	This study
Spring	Yanzhou	8.6 ± 3.3	6.8 ± 2.5	3.1 ± 1.4	2.2 ± 0.4	2.9 ± 0.5	
Summer	Yanzhou	8.0 ± 2.9	6.7 ± 2.5	4.5 ± 2.2	2.0 ± 0.3	2.3 ± 0.4	
Autumn	Yanzhou	10.9 ± 4.7	8.8 ± 3.6	3.5 ± 1.9	3.5 ± 0.8	4.6 ± 1.1	
Winter	Yanzhou	19.5 ± 9.4	15.1 ± 7.0	4.2 ± 2.3	4.8 ± 1.1	7.4 ± 1.7	
Annual (2018–2019)	Lanzhou		6.4 ± 4.5	2.5 ± 1.8	2.0 ± 1.3		Chen et al. (2023)
Spring (2018–2019)	Lanzhou		4.5 ± 1.9	2.1 ± 1.2	1.4 ± 0.6		
Summer (2018–2019)	Lanzhou		3.5 ± 1.0	1.3 ± 0.6	1.6 ± 0.6		
Autumn (2018–2019)	Lanzhou		7.1 ± 4.3	3.6 ± 2.5	2.6 ± 1.5		
Winter (2018–2019)	Lanzhou		10.0 ± 5.1	3.0 ± 1.3	2.4 ± 1.5		
Annual (2016–2017)	Beijing		11.0 ± 10.7		3.4 ± 3.3		Ji et al. (2019)
Annual (2016–2017)	Tianjing		12.0 ± 9.8		3.1 ± 3.6		
Annual (2016–2017)	Shijiazhuang		22.8 ± 30.6		5.4 ± 6.5		
Annual (2016–2017)	Tangshan		12.1 ± 9.6		3.5 ± 3.6		
Winter 2019–2022	Guangzhou	10.9 ± 6.1	8.6 ± 4.7	2.8 ± 1.9	4.7 ± 3.2		Huang et al. (2022)
Winters (2015–2017)	Shanghai		7.3 ± 4.5		3.8 ± 2.4		Yao et al. (2020)
Annual (2018–2020)	Los Angeles Basin	3.7 ± 1.2			0.9 ± 0.4		Ivančič et al. (2022)
Annual (2018–2019)	Augsburg				1.1 ± 1.0		Liu et al. (2022)
Annual (2015–2018)	Elche		5.9 ± 2.2		1.2 ± 0.5		Galindo et al. (2019)

AT, RH, WD, WS, PP, and HPBL) were examined by Random Forest Regression Analyses using a package Scikit-Learn (python 3.6). Briefly, for a given season, 70% of the monitoring data was selected as the training data, and the 5-fold CV method was used to estimate the accuracy of the method, where the data set is randomly separated to 5 partitions with equal-sized folds. The algorithm is trained using fourfold and repeated 5 times. The graphs in this study were processed using OriginPro 2021b (OriginLab Corporation, Northampton, MA, USA.)

3. Results and discussion

3.1. Carbonaceous aerosols levels

The mean concentrations of TC, OC, SOC, eBC, and eUVBC in Yanzhou reached 11.1 ± 6.7, 8.9 ± 5.1, 3.9 ± 2.0, 3.1 ± 1.3, and 4.3 ± 2.4 μg/m^3, respectively (Table 1), accounting for 26.8% ± 24.5%, 22.1% ± 23.5%, 12.6% ± 16.6%, 6.6% ± 1.3%, and 8.7% ± 1.0% of the $PM_{2.5}$ mass during the sampling period. The concentrations of TC, OC, and eBC in Yanzhou were similar to those reported for Guangzhou (Huang et al., 2022) and much lower than those for Beijing-Tianjin-Shijiazhuang region (Ji et al., 2019), but were higher than those in Lanzhou of northwest China (Chen et al., 2023) and

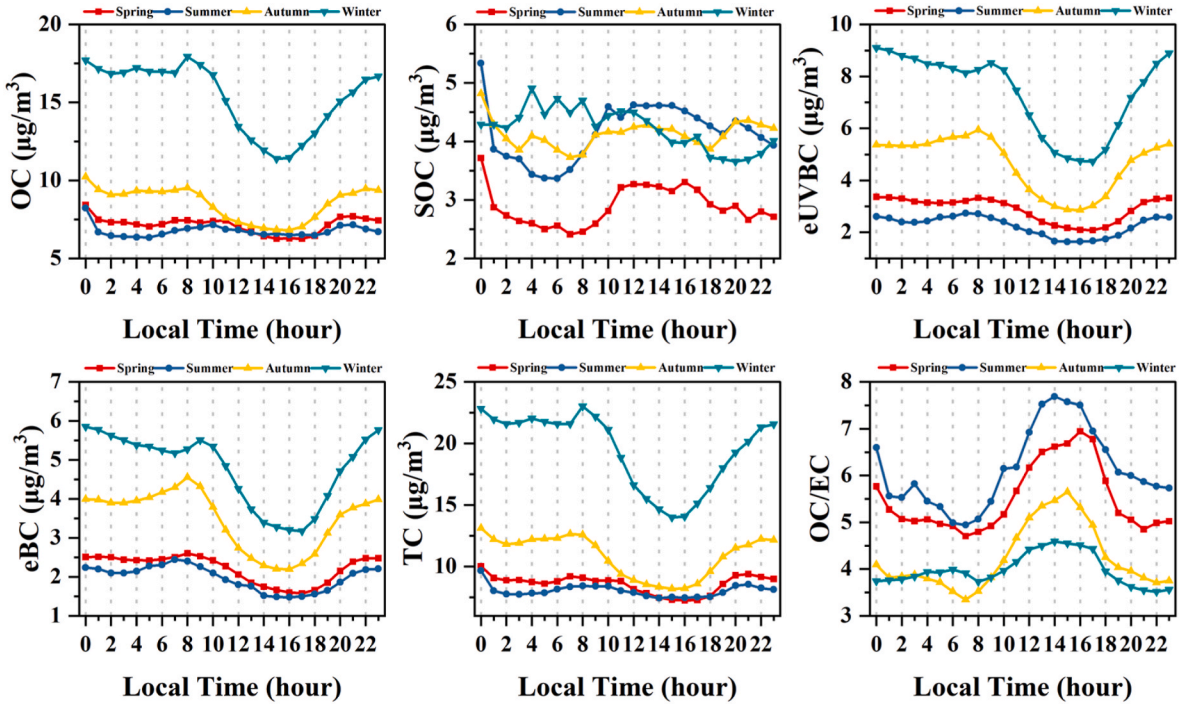

Fig. 1. Diels of various carbonaceous aerosols in Yanzhou, plotted as season averages (TC, OC, and SOC monitored during 2019–2020, and eBC and eUVBC monitored during 2019–2022).

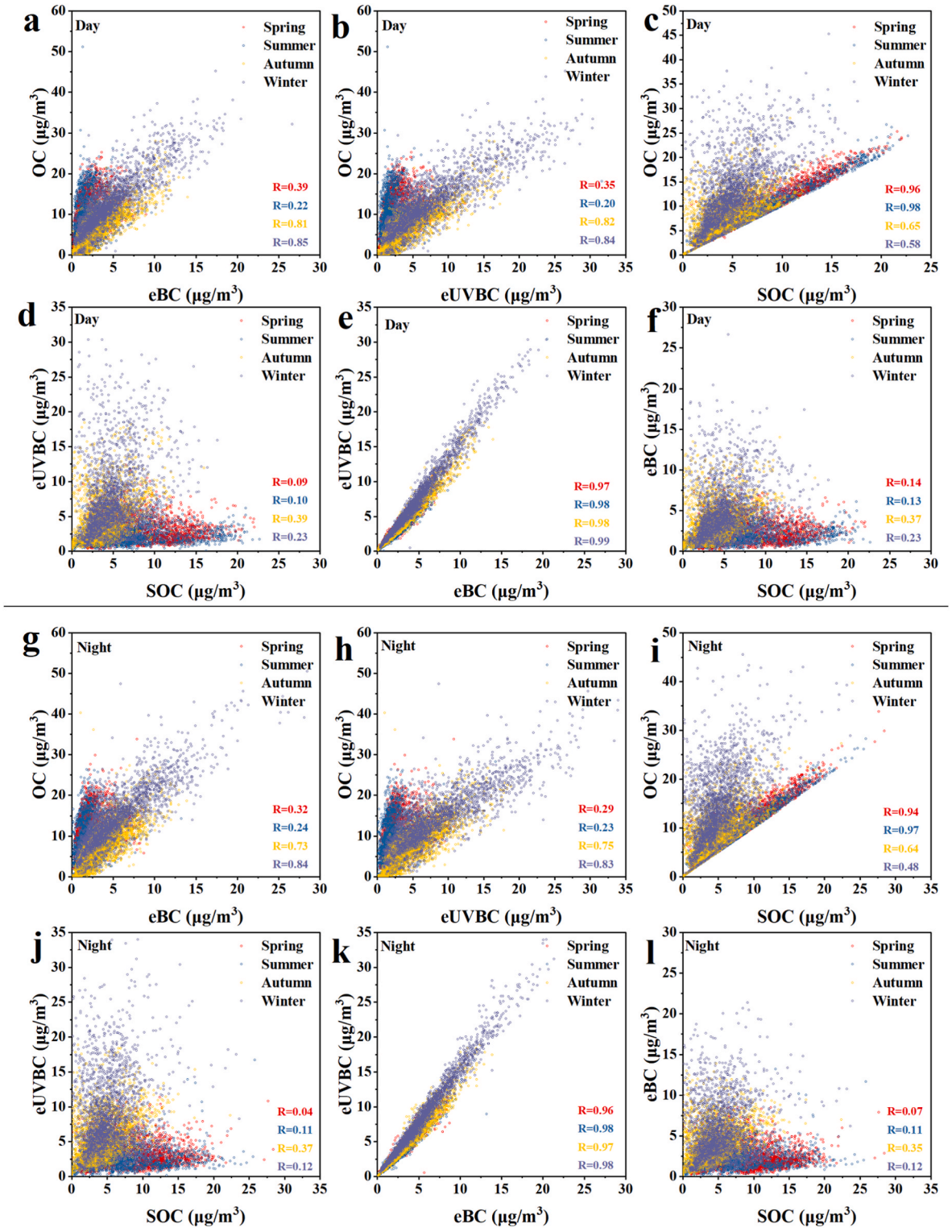

Fig. 2. Cross correlation plots among components of the carbonaceous aerosol during daytime (06:00–17:00 LT: a-f) and nighttime (18:00–05:00 LT: g-l) (TC, OC, and SOC monitored during 2019–2020, and eBC and eUVBC monitored during 2019–2022).

Shanghai of the Yangtze River Delta region in recent years (Yao et al., 2020). This indicates that Yanzhou, as a northern Chinese city, has an intermediate concentration of carbonaceous aerosols in urban China. Nonetheless, concentrations in this region tend to exceed those observed in Western cities like Los Angeles, USA (Ivančič et al., 2022); Augsburg, Germany (Liu et al., 2021); and Elche, Spain (Galindo et al., 2019). Hence, it remains imperative to implement more precise control measures to ameliorate air quality and safeguard environmental health.

The OC/EC might change according the origin and source contribution of these two components, and affects absorption by aerosols. Thus, OC/EC is used as an important diagnostic index for reflecting the type and source contribution of carbonaceous aerosols, with higher OC/EC ratios typically indicating greater contributions from biomass burning sources and secondary organic aerosols (SOA), and lower ones

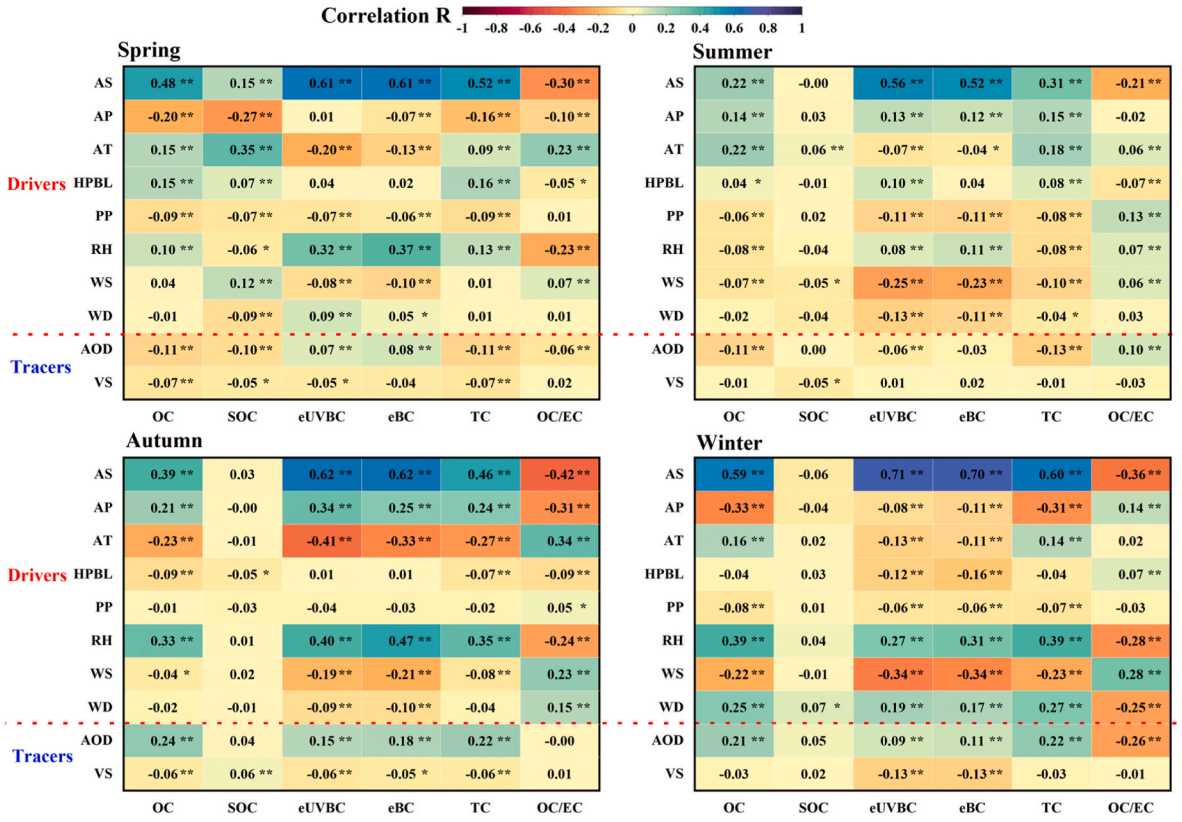

Fig. 3. Pearson's correlation coefficients matrix of meteorological drivers and tracers and major components of carbonaceous aerosol (drivers: AS, atmospheric stability; AP, air pressure; AT, air temperature; HPBL, height planetary boundary layer; PP, precipitation; RH, relative humidity; WS, wind speed; and WD, wind direction; tracers: AOD, aerosol optical depth and VS, visibility. *p < 0.05, **p < 0.01).

indicating greater contributions from fossil fuel combustion sources (Turpin and Lim, 2001). In general, biomass burning has a higher OC/EC ratio than fossil fuel combustion, and therefore urban areas usually have lower OC/EC ratios (1.0–4.0) than rural or remote regions (Kunwar and Kawamura, 2014). Furthermore, high contributions of SOA will increase SOA and OC, because EC is not supplied in this case. In this study, the OC/EC ratios varied from 1.7 to 14.8, with an average of 5.0 ± 2.2. Meanwhile, the OC/EC ratio showed high levels in all seasons, indicating the significant contribution of SOA. The seasonal mean OC/EC was highest in summer (6.1 ± 0.8), followed by spring (5.5 ± 0.7), autumn (4.2 ± 0.7) and winter (4.0 ± 0.3). The annual mean OC/EC (5.0 ± 1.1) was similar to those derived in several urban areas in China, such as Lanzhou (Chen et al., 2023), Beijing (Ji et al., 2019), Zhengzhou (Wang et al., 2017), Shanghai (Xu et al., 2018), which are significantly affected by biomass burning emission and SOA formation (Zhang et al., 2007).

3.2. Temporal variations

Fig. 1 shows the diurnal variations of OC, SOC, eUVBC, eBC, and TC, and OC/EC under four seasons. The results show that carbonaceous aerosol concentrations were higher during nighttime (18:00–05:00 LT) when compared with daytime (6:00–17:00 LT) in all seasons, pointing to the HPBL as a major driver. The low nocturnal HPBL and stable atmospheric conditions reduced the vertical and horizontal dispersion of pollutants, thus leading to the accumulation of pollutants in the inversion layer (Liu et al., 2022).

For OC, eUVBC, eBC, and TC, distinct morning peaks can be observed during autumn and winter, while the weaker morning peaks occur in spring and summer (Fig. 1). These peaks were typically observed ~ 1–2 h after sunrise (08:00–09:00 LT). The presence of increased vehicular emissions throughout the year, as well as the cold starts specifically during autumn and winter, were both likely contributing factors to these patterns. However, as the HPBL increases, as wind speed does, in midday, the concentrations of these aerosols were diluted. In the afternoon (16:00–17:00 LT), the lowest levels of OC, eUVBC, eBC, and TC were observed due to the increased atmospheric ventilation and still relatively high HPBL. Subsequently, a night peak regularly occurred between 22:00 and 00:00 LT, as linked to various factors such as evening traffic rush-hours, the increase of household heating, coal and natural gas burning (especially in winter), and the unfavorable meteorological conditions. From midnight to early morning (01:00 to 07:00 LT), there was a slight decreasing trend, which can be attributed to the reduction in anthropogenic emissions and some dry deposition of near-surface PM occurring at low wind speeds.

Since the SOA formation requires the presence of solar radiation (Peng et al., 2021), the daytime OC/EC was higher than that in nighttime, and generally peaks at 14:00–16:00 LT alongside the highest irradiance. The average ratios were 5.7 ± 1.7, 6.3 ± 2.8, 4.5 ± 1.7, and 4.2 ± 1.1 during the daytime, while in the nighttime were 5.3 ± 1.6, 6.0 ± 2.9, 4.0 ± 1.4, and 3.8 ± 1.1 for spring, summer, autumn, and winter, respectively. Typical characteristic values for OC/EC ratios have been identified for various sources, including gasoline and diesel vehicle exhaust with a ratio range of 1.0–4.2 (Schauer et al., 2001, 2002a), biomass combustion with a ratio range of 16.8–40.0 (Schauer et al., 2002b), coal combustion with a ratio range of 2.5–10.6 (Chen et al., 2006), cooking emissions with characteristic ratio values ranging from 32.8 to 81.7 (He et al., 2004), ground dust with a ratio value of 13.1 (Zhang et al., 2007), and household natural gas with a ratio value of 12.7 (Chow et al., 1996). However, we have to consider that the SOA formation contributes to OC without EC. Therefore, in summer, the higher OC/EC values implied that some other sources, such as SOA formation, biomass burning and cooking, may contribute to the considerable amount of atmospheric carbonaceous aerosols. While in other seasons,

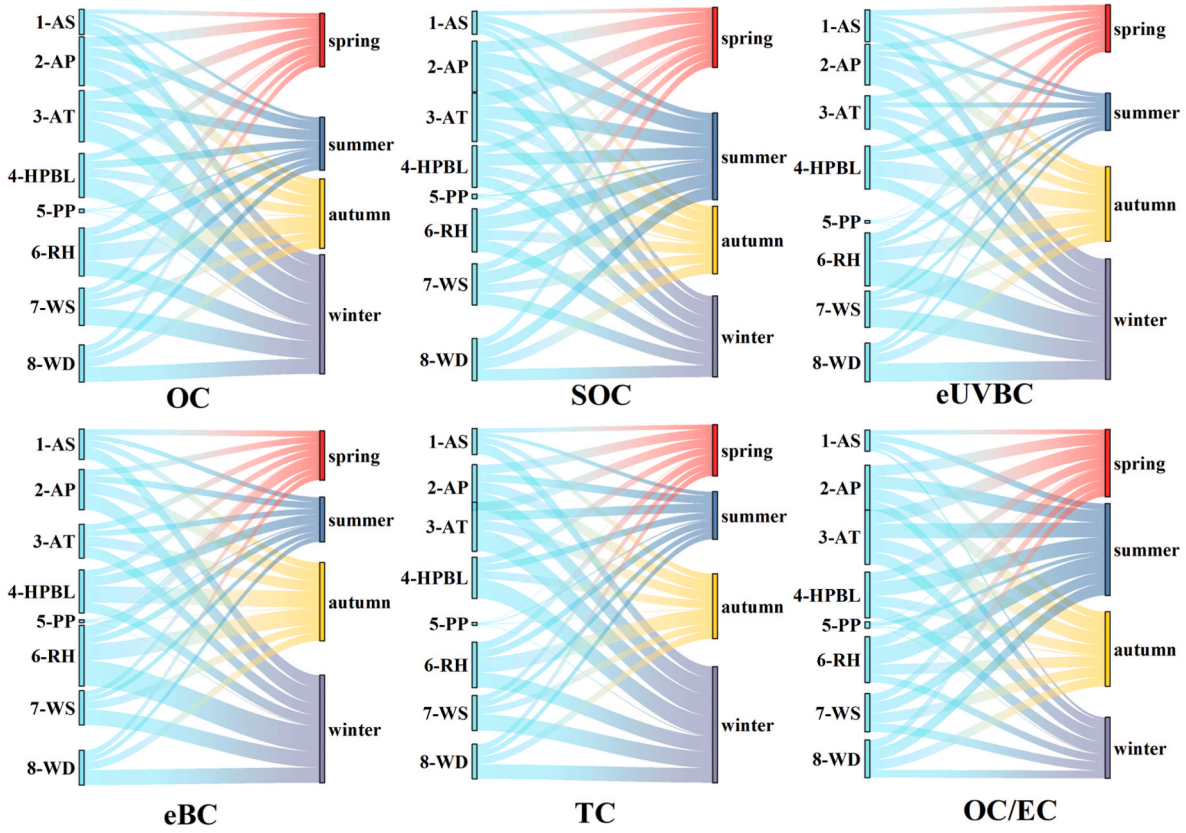

Fig. 4. Identification of driving factor of the carbonaceous aerosol components based on the Random Forest analysis in Yanzhou during different seasons (AS, atmospheric stability; AP, air pressure; AT, air temperature; HPBL, height planetary boundary layer. PP, precipitation; RH, relative humidity; WS, wind speed; and WD, wind direction).

the carbonaceous aerosols in Yanzhou's atmosphere could be highly associated with coal combustion in all seasons, in line with the abundant local coal production (Xiao et al., 2018).

3.3. Correlations among carbonaceous constituents

As shown by Fig. 2, the correlations among SOC, eUVBC, eBC, and OC were generally higher during daytime than nighttime in all seasons, except summers. This suggests that carbonaceous aerosols are more influenced by combustion activity during the daytime, in line with the fact that traffic emissions are more significant during the daytime. By contrast, during summer nights, more significant photochemistry, i.e., the increased reactions and accelerated kinetics induced by sunlight irradiation, may contribute largely to the secondary carbonaceous components (George et al., 2015), together with the increased local combustion activities (*e.g.*, open-air barbecue) as another potential contributor to both primary and secondary aerosol species.

Moreover, by examining the correlation between OC and eBC (Fig. 2 a and g), it is possible to gain insight into the coherence of their origins because a significant correlation normally indicates the similar sources (Liu et al., 2021). In brief, eBC is primarily emitted from the incomplete combustion of fossil and non-fossil fuels, and remain relatively stable, while the sources of OC are diverse, including both primary OC emissions and SOC (Bond et al., 2013; Hallquist et al., 2009). Fig. 2 shows that during spring and summer, the correlation between OC and eBC was low both day and night, whereas during autumn and winter, the correlation between day and night was high ($R > 0.7$, $p < 0.01$). This suggests that the OC and eBC in the cold seasons were derived mostly from consistent primary emissions, whereas the sources in the warm seasons of the PM components were different the low concentration decreased their relationship.

The correlations between OC and SOC in spring and summer were higher than that in autumn and winter (Fig. 2 c and i), suggesting that SOC is the main part of OC in spring and summer. Taking in mind the above heterogenous monthly patterns among seasons, SOC made up varied proportions of OC: 40.5% in spring, 59.6% in summer, 46.8% in autumn, and 25.8% in winter. The lowest winter SOC to OC contributions was most probably due to the unfavorable conditions for SOC formation, such as low temperatures (averaging around 2.5 °C–8.6 °C) and reduced sunlight irradiance (Cao et al., 2007). On the other hand, the highest summer SOC contribution was consistent with the most favorable conditions for photochemistry and the lower contribution from coal combustion (Xie et al., 2019).

3.4. Major drivers of the carbonaceous aerosols

The correlations between different carbonaceous aerosols and the drivers (AS, AP, AT, RH, WD, WS, PP, PBL, and VS) or tracers (AOD and VS) were evaluated. As shown in Fig. 3, the correlations between meteorological factors and carbonaceous aerosols were highly significant in four seasons ($p < 0.01$). As it could be expected from the findings described in the prior sections, these correlations varied with seasons (Fig. 3). For instance, RH had a significant positive correlation with OC concentrations in winter but negative in summer with OC and SOC (Fig. 3).

However, some uncertainties may exist in the correlation analysis. For instance, some factors may follow a nonlinear association that cannot be accurately characterized by common correlation analysis methods. Accordingly, machine learning method, *e.g.*, random forest regression analysis, can be used to reveal more potential associations among these factors, followed by the outcome of quantitative importance scores (Fig. 4). As seen from the results, the drivers for each

Table 2
Main drivers (+) for different carbonaceous aerosols and OC/EC in different seasons. In this study, factors with weights greater than 0.15 were defined as the main drivers.

Season	Drivers	OC	SOC	eUVBC	eBC	TC	OC/EC
Spring	AS						
	AP	+	+			+	+
	AT	+	+			+	+
	HPBL						
	PP						
	RH	+		+	+	+	+
	WS						
	WD						
Summer	AS						
	AP	+	+		+	+	
	AT	+	+		+	+	+
	HPBL			+	+		+
	PP						
	RH	+	+		+	+	+
	WS		+				
	WD						+
Autumn	AS						
	AP	+	+	+		+	+
	AT	+	+			+	+
	HPBL			+	+		
	PP						
	RH	+	+	+	+	+	
	WS						
	WD		+				
Winter	AS						
	AP	+	+	+	+	+	+
	AT	+	+			+	+
	HPBL	+				+	+
	PP						
	RH		+	+	+		
	WS	+		+	+		
	WD			+			

carbonaceous aerosol component were evaluated varying with seasons. When constructing each decision tree, the Random Forest algorithm randomly samples each variable and ranks them based on their importance. Importance is typically measured by calculating the sum of information gain or Gini coefficient for each variable throughout the tree-building process. These metrics indicate the contribution of each variable to the decision tree's predictions.

The main drivers influencing all types of carbonaceous aerosols and OC/EC, encompass the variables of HPBL, AT, RH, and AP, and this relationship holds true across all seasons (Fig. 4). However, the relative impact of these key meteorological drivers on each specific type of carbonaceous aerosol exhibits seasonal variation, as outlined in Table 2. HPBL exerts a crucial influence on the vertical distribution and diffusion of carbonaceous aerosols (Lu et al., 2020). Elevated HPBL facilitates aerosol mixing and diffusion, resulting in reduced concentrations. This demonstrates a non-linear relationship wherein changes in HPBL may not yield proportional changes in aerosol levels. Moreover, AT plays a pivotal role in enhancing aerosol volatility and influencing aerosol-gas interactions (Paasonen et al., 2013). This dynamic leads to consequential effects on the chemical reactions and formation processes of carbonaceous aerosols. It is important to note that these interactions may not always follow a straightforward, linear pattern, further underscoring the non-linearity in the relationship. RH introduces another layer of complexity, impacting both moisture absorption and particle size of carbonaceous aerosols (Hems et al., 2021). In conditions of higher RH, carbonaceous aerosols have a propensity to absorb moisture and enlarge in size. This subsequently leads to alterations in their optical properties and scattering abilities. Additionally, elevated RH can foster the formation of SOA, thereby influencing the composition and concentration of aerosols in the atmosphere (Li et al., 2017; Y. Liu et al., 2018). Furthermore, variations in AP can affect aerosol density and concentration distribution (Yang et al., 2022). A higher AP can accelerate the deposition rate of carbonaceous aerosols and augment the flux of settling particles towards the ground.

It is essential to recognize that these factors engage in intricate interactions, further influenced by other atmospheric conditions such as WS. Consequently, the behavior and distribution of carbonaceous aerosols emerge as the outcome of multifaceted interplays among these variables. The nuanced composition and abundance of carbonaceous aerosols witnessed in distinct seasons underscore the need to consider specific meteorological drivers in seasonal analyses. This recognition emphasizes the critical importance of accounting for seasonal variations when investigating the impact of carbonaceous aerosols on air quality and climate. By discerning these seasonal distinctions, scientists and policymakers can craft targeted strategies to effectively mitigate and manage carbonaceous aerosol pollution.

In addition, for the tracer factors (AOD and VS), two obvious indicators of air quality (Kumar et al., 2011; Molnar et al., 2020), their larger relationship with each carbonaceous aerosol indicates the affection of carbonaceous aerosols on AOD and VS, which will facilitate the application of AOD and VS inversion for carbonaceous aerosols.

3.5. Assessment of eBC-associated health risk

Population is exposed to atmospheric eBC primarily through inhalation of air in the vicinity of local or regional sources. Because both air pollution and ETS are exposed by inhalation and are largely involuntary, and exposure to complex mixtures of particles and gases have similar health effects, the health risks of exposure to air pollution and equivalent NPSC are considered to be comparable in terms of health risk (Wu et al., 2018). As stated above, the health risk assessment model has been applied by prior studies to use four health endpoints, including LBW, LC, CM, and PLFD for evaluating potential health risks of eBC exposure (van der Zee et al., 2016), and expressed into equivalent NPSC, which has been adapted in this study.

Using the eBC of Yanzhou during the 3.5 years, the eBC health risks expressed by NPSC were obtained. The characteristics of the NPSC for the four health points in the different seasons are obviously consistent with those of the eBC levels (winter > autumn > spring > summer) (Fig. 5) and showed significant seasonal differences ($p < 0.01$). In general, during the observed periods (August 2019 to December 2022), the average health risks values of LBW, LC, CM, and PLFD reached 8.6 ± 6.1, 4.1 ± 2.9, 25.8 ± 18.2, and 9.1 ± 6.4 equivalent numbers of PSC, respectively. These values were similar with Xining, China (Wu et al., 2018), lower than that in Beijing, China (Ji et al., 2017), Delhi, India (Srivastava et al., 2014), but were still higher than those in European and American cities including (*e.g.*, Stockholm, Sweden (Krecl et al., 2017), Ny-Ålesund, Norway (Markowicz et al., 2017), Augsburg, Germany (Liu et al., 2022) and Los Angeles, USA (Krasowsky et al., 2016)). It has been reported that the health risks exposure to 1 $\mu g/m^3$ of eBC were equivalent to 4 PSC per day across the four health outcomes (van der Zee et al., 2016), which was lower than the overall estimated health risks of eBC in Yanzhou, indicating a high health risk in the area. In particular, the effects of eBC exposure on lung function in school-age children are higher than the adverse effects on cardiovascular and lung disease in adults, making children a vulnerable and health-vulnerable group in eBC pollution-exposed environments, demonstrating the relatively high health risk loss to children from increased eBC and the urgency and need for municipalities to step up efforts to combat and mitigate eBC in the environment.

4. Conclusions

Exposure to carbonaceous aerosols has remained a significant environmental concern in urban areas. This study conducted a comprehensive analysis of multi-year temporal variations of carbonaceous aerosols, encompassing OC, SOC, eUVBC, eBC, and TC, in urban Yanzhou. The

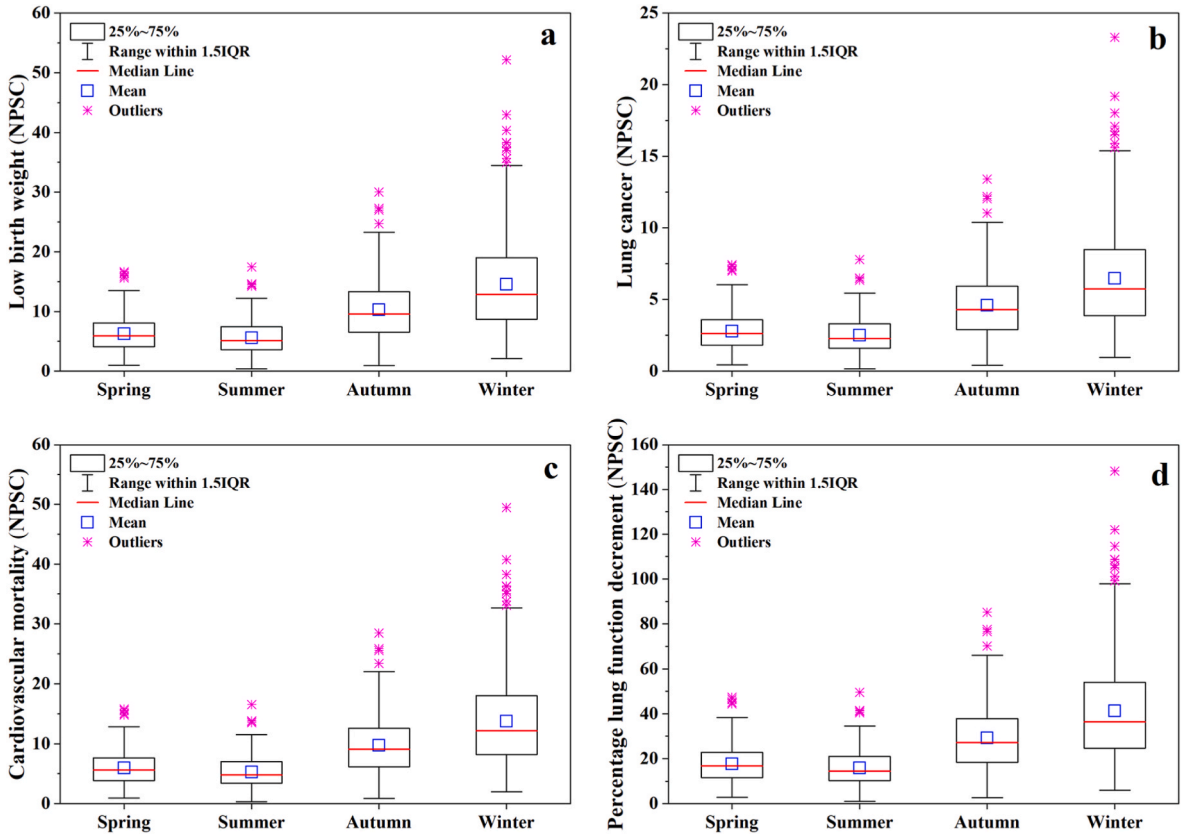

Fig. 5. Box plots of health risks of equivalent black carbon (eBC) were evaluated by (a) low birth weight (LBW), (b) lung cancer (LC), and (c) cardiovascular mortality (CM), (d) percentage lung function decrement of school aged children (PLFD), and expressed into equivalent numbers of passively smoked cigarettes (NPSC) during four seasons in Yanzhou.

diurnal and seasonal variability of these aerosols exhibited noteworthy disparities, attributable to alterations in emission rates, atmospheric mixing and dispersion conditions, as well as boundary-layer dynamics. Notably, the variables of HPBL, AT, RH, and AP emerged as primary drivers of carbonaceous aerosols. Therefore, subsequent modeling studies should place particular emphasis on analyzing periods with significant variations in factors identified as having high importance scores, offering deeper insights into carbonaceous pollution dynamics. A more comprehensive examination of emission sources necessitates the incorporation of additional chemical indicators (*e.g.*, inorganic salt ions), which are recommended for future research. Meanwhile, the correlational analysis shed light on potential sources of carbonaceous aerosols, underscoring the need for additional control measures. Given that major sources may vary seasonally, it is imperative to tailor response strategies to specific circumstances. Furthermore, the health analysis indicated that a certain demographic group, represented by school-age children faces the highest health risks. This underscores the importance for governmental authorities to implement targeted measures for this particular demographic, ensuring the safeguarding of public health.

In summary, this research addresses a gap in atmospheric environmental studies for Yanzhou and its surrounding regions, providing valuable insights through on-site observations. It calls for future studies to employ high spatiotemporal resolution models specific to this area for a more comprehensive understanding. The integration of machine learning techniques and in-depth analysis of influential factors will enhance our grasp of carbonaceous pollution patterns. The identification of specific sources through correlational analysis emphasizes the need for tailored control strategies. Finally, the health analysis underscores the necessity for targeted interventions, particularly for children. These findings collectively contribute to a more thorough and comprehension of carbonaceous aerosol pollution and pave the way for the development of effective management strategies.

CRediT authorship contribution statement

Xiansheng Liu: Data curation, Methodology, Software, Writing – original draft. **Xun Zhang:** Software. **Bowen Jin:** Methodology. **Hadiatullah Hadiatullah:** Methodology, Software. **Luyao Zhang:** Writing – original draft. **Pei Zhang:** Writing – original draft. **Tao Wang:** Supervision, Writing – review & editing. **Qihong Deng:** Writing – review & editing. **Xavier Querol:** Writing – review & editing.

Declaration of competing interest

The authors declare that they have no known competing financial interests or personal relationships that could have appeared to influence the work reported in this paper.

Data availability

Data will be made available on request.

Acknowledgements

This study is supported by the RI-URBANS project (Research Infrastructures Services Reinforcing Air Quality Monitoring Capacities in European Urban & Industrial Areas, European Union's Horizon 2020 research and innovation program, Green Deal, European Commission, contract 101036245). This study is also supported by National Natural Science Foundation of China (42101470, 72242106, 42205099), Xinjiang Autonomous Region Social Science Foundation Project

(2023BTY128) and China Postdoctoral Science Foundation (2021M700792), Project of Natural Science Foundation of Xinjiang Uygur Autonomous Region (2023D01A57), and in part by the Chunhui Project Foundation of the Education Department of China under Grant HZKY20220053.

Appendix A. Supplementary data

Supplementary data to this article can be found online at https://doi.org/10.1016/j.atmosenv.2023.120169.

References

Ali, M.U., Siyi, L., Yousaf, B., Abbas, Q., Hameed, R., Zheng, C., Kuang, X., Wong, M.H., 2021. Emission sources and full spectrum of health impacts of black carbon associated polycyclic aromatic hydrocarbons (PAHs) in urban environment: a review. Crit. Rev. Environ. Sci. Technol. 51, 857–896.

Alves, C., Vicente, A., Pio, C., Kiss, G., Hoffer, A., Decesari, S., Prevôt, A.S., Minguillón, M.C., Querol, X., Hillamo, R., 2012. Organic compounds in aerosols from selected European sites–Biogenic versus anthropogenic sources. Atmos. Environ. 59, 243–255.

Bond, T.C., Doherty, S.J., Fahey, D.W., Forster, P.M., Berntsen, T., DeAngelo, B.J., Zender, C.S., 2013. Bounding the role of black carbon in the climate system: a scientific assessment. J. Geophys. Res. Atmos. 11, 5380–5552.

Brokamp, C., Jandarov, R., Rao, M.B., LeMasters, G., Ryan, P., 2017. Exposure assessment models for elemental components of particulate matter in an urban environment: a comparison of regression and random forest approaches. Atmos. Environ. 1–11.

Cao, J.J., Lee, S.C., Chow, J.C., Watson, J.G., Ho, K.F., Zhang, R.J., Jin, Z.D., Shen, Z.X., Chen, G.C., Kang, Y.M., 2007. Spatial and seasonal distributions of carbonaceous aerosols over China. J. Geophys. Res. Atmos. 112.

Castro, L.M., Pio, C.A., Harrison, R.M., Smith, D., 1999. Carbonaceous aerosol in urban and rural European atmospheres: estimation of secondary organic carbon concentrations. Atmos. Environ. 33, 2771–2781.

Chen, Y., Zhi, G., Feng, Y., Fu, J., Feng, J., Sheng, G., Simoneit, B.R., 2006. Measurements of emission factors for primary carbonaceous particles from residential raw-coal combustion in China. Geophys. Res. Lett. 33.

Chen, W., Tian, H., Zhao, H., Qin, K., 2020. Multichannel characteristics of absorbing aerosols in Xuzhou and implication of black carbon. Sci. Total Environ. 714, 136820.

Chen, P., Kang, S., Gan, Q., Yu, Y., Yuan, X., Liu, Y., Tripathee, L., Wang, X., Li, C., 2023. Concentrations and light absorption properties of PM2. 5 organic and black carbon based on online measurements in Lanzhou, China. J. Environ. Sci. (China) 131, 84–95.

Cheng, Y., He, K., Zheng, M., Duan, F., Du, Z., Ma, Y., Tan, J., Yang, F., Liu, J., Zhang, X., 2011. Mass absorption efficiency of elemental carbon and water-soluble organic carbon in Beijing, China. Atmos. Chem. Phys. 11, 11497–11510.

Chow, J.C., Watson, J.G., Lu, Z., Lowenthal, D.H., Frazier, C.A., Solomon, P.A., Thuillier, R.H., Magliano, K., 1996. Descriptive analysis of PM2. 5 and PM10 at regionally representative locations during SJVAQS/AUSPEX. Atmos. Environ. 30, 2079–2112.

Colbeck, I., Lazaridis, M., 2010. Aerosols and environmental pollution. Naturwissenschaften 97, 117–131.

Dai, T., Dai, Q., Ding, J., Liu, B., Bi, X., Wu, J., Zhang, Y., Feng, Y., 2023. Measuring the emission changes and meteorological dependence of source-specific BC aerosol using factor analysis coupled with machine learning. e2023J J. Geophys. Res. Atmos. 128, e38696J.

Dong, Z., Wang, S., Sun, J., Shang, L., Li, Z., Zhang, R., 2022. Impact of COVID-19 lockdown on carbonaceous aerosols in a polluted city: composition characterization, source apportionment, influence factors of secondary formation. Chemosphere 307, 136028.

Duan, F., He, K., Ma, Y., Jia, Y., Yang, F., Lei, Y., Tanaka, S., Okuta, T., 2005. Characteristics of carbonaceous aerosols in Beijing, China. Chemosphere 60, 355–364.

Dumka, U.C., Tiwari, S., Kaskaoutis, D.G., Soni, V.K., Safai, P.D., Attri, S.D., 2019. Aerosol and pollutant characteristics in Delhi during a winter research campaign. Environ. Sci. Pollut. Res. Int. 26, 3771–3794.

Esposito, F., 2012. Interactive comment on "A new algorithm for brown and black carbon identification and organic carbon detection in fine atmospheric aerosols by a multi-wavelength Aethalometer" by F. Esposito et al.

Galindo, N., Yubero, E., Clemente, A., Nicolás, J.F., Navarro-Selma, B., Crespo, J., 2019. Insights into the origin and evolution of carbonaceous aerosols in a mediterranean urban environment. Chemosphere 235, 636–642.

George, C., Ammann, M., D Anna, B., Donaldson, D.J., Nizkorodov, S.A., 2015. Heterogeneous photochemistry in the atmosphere. Chem. Rev. 115, 4218–4258.

Gilardoni, S., Vignati, E., Marmer, E., Cavalli, F., Belis, C., Gianelle, V., Loureiro, A., Artaxo, P., 2011. Sources of carbonaceous aerosol in the Amazon basin. Atmos. Chem. Phys. 11, 2747–2764.

Glasius, M., Hansen, A., Claeys, M., Henzing, J.S., Jedynska, A.D., Kasper-Giebl, A., Kistler, M., Kristensen, K., Martinsson, J., Maenhaut, W., 2018. Composition and sources of carbonaceous aerosols in Northern Europe during winter. Atmos. Environ. 173, 127–141.

Hallquist, M., Wenger, J.C., Baltensperger, U., Rudich, Y., Simpson, D., Claeys, M., Dommen, J., Donahue, N.M., George, C., Goldstein, A.H., 2009. The formation, properties and impact of secondary organic aerosol: current and emerging issues. Atmos. Chem. Phys. 9, 5155–5236.

He, L., Hu, M., Huang, X., Yu, B., Zhang, Y., Liu, D., 2004. Measurement of emissions of fine particulate organic matter from Chinese cooking. Atmos. Environ. 38, 6557–6564.

Hems, R.F., Schnitzler, E.G., Liu-Kang, C., Cappa, C.D., Abbatt, J.P., 2021. Aging of atmospheric brown carbon aerosol. ACS Earth Space Chem. 5, 722–748.

Hopke, P.K., Ito, K., Mar, T., Christensen, W.F., Eatough, D.J., Henry, R.C., Kim, E., Laden, F., Lall, R., Larson, T.V., 2006. PM source apportionment and health effects: 1. Intercomparison of source apportionment results. J. Expo. Sci. Environ. Epidemiol. 16, 275–286.

Hopkins, R.J., Tivanski, A.V., Marten, B.D., Gilles, M.K., 2007. Chemical bonding and structure of black carbon reference materials and individual carbonaceous atmospheric aerosols. J. Aerosol Sci. 38, 573–591.

Huang, J., Zhang, Z., Tao, J., Zhang, L., Nie, F., Fei, L., 2022. Source apportionment of carbonaceous aerosols using hourly data and implications for reducing PM2. 5 in the Pearl River Delta region of South China. Environ. Res. 210, 112960.

IARC, 2012. Diesel and gasoline engine exhausts and some nitroarenes. IARC (Int. Agency Res. Cancer) Monogr. Eval. Carcinog. Risks Hum. 105, 978-92-832-1210-2. 2012.

Ivančič, M., Gregorič, A., Lavrič, G., Alföldy, B., Ježek, I., Hasheminassab, S., Pakbin, P., Ahangar, F., Sowlat, M., Boddeker, S., 2022. Two-year-long high-time-resolution apportionment of primary and secondary carbonaceous aerosols in the Los Angeles Basin using an advanced total carbon–black carbon (TC-BC (λ)) method. Sci. Total Environ. 848, 157606.

Janssen, N.A., Gerlofs-Nijland, M.E., Lanki, T., Salonen, R.O., Cassee, F., Hoek, G., Fischer, P., Brunekreef, B., Krzyzanowski, M., 2012. Health Effects of Black Carbon. WHO.

Ji, D., Li, L., Pang, B., Xue, P., Wang, L., Wu, Y., Zhang, H., Wang, Y., 2017. Characterization of black carbon in an urban-rural fringe area of Beijing. Environ. Pollut. 223, 524–534.

Ji, D., Gao, M., Maenhaut, W., He, J., Wu, C., Cheng, L., Gao, W., Sun, Y., Sun, J., Xin, J., 2019. The carbonaceous aerosol levels still remain a challenge in the Beijing-Tianjin-Hebei region of China: insights from continuous high temporal resolution measurements in multiple cities. Environ. Int. 126, 171–183.

Jimenez, J.L., Canagaratna, M.R., Donahue, N.M., Prevot, A., Zhang, Q., Kroll, J.H., DeCarlo, P.F., Allan, J.D., Coe, H., Ng, N.L., 2009. Evolution of organic aerosols in the atmosphere. Science 326, 1525–1529.

Krasowsky, T.S., McMeeking, G.R., Wang, D., Sioutas, C., Ban-Weiss, G.A., 2016. Measurements of the impact of atmospheric aging on physical and optical properties of ambient black carbon particles in Los Angeles. Atmos. Environ. 142, 496–504.

Krecl, P., Johansson, C., Targino, A.C., Ström, J., Burman, L., 2017. Trends in black carbon and size-resolved particle number concentrations and vehicle emission factors under real-world conditions. Atmos. Environ. 165, 155–168.

Kumar, N., Chu, A.D., Foster, A.D., Peters, T., Willis, R., 2011. Satellite remote sensing for developing time and space resolved estimates of ambient particulate in Cleveland, OH. Aerosol. Sci. Technol. 45, 1090–1108.

Laskin, A., Laskin, J., Nizkorodov, S.A., 2015. Chemistry of atmospheric brown carbon. Chem. Rev. 115, 4335–4382.

Li, Z., Guo, J., Ding, A., Liao, H., Liu, J., Sun, Y., Wang, T., Xue, H., Zhang, H., Zhu, B., 2017. Aerosol and boundary-layer interactions and impact on air quality. Natl. Sci. Rev. 4, 810–833.

Li, C., Yan, F., Kang, S., Yan, C., Hu, Z., Chen, P., Gao, S., Zhang, C., He, C., Kaspari, S., 2021. Carbonaceous matter in the atmosphere and glaciers of the Himalayas and the Tibetan plateau: an investigative review. Environ. Int. 146, 106281.

Liu, Q., Jia, X., Quan, J., Li, J., Li, X., Wu, Y., Chen, D., Wang, Z., Liu, Y., 2018. New positive feedback mechanism between boundary layer meteorology and secondary aerosol formation during severe haze events. Sci. Rep. 8, 1–8.

Liu, Y., Yan, C., Zheng, M., 2018. Source apportionment of black carbon during winter in Beijing. Sci. Total Environ. 618, 531–541.

Liu, X., Hadiatullah, H., Tai, P., Xu, Y., Zhang, X., Schnelle-Kreis, J., Schloter-Hai, B., Zimmermann, R., 2021. Air pollution in Germany: spatio-temporal variations and their driving factors based on continuous data from 2008 to 2018. Environ. Pollut. 276, 116732.

Liu, X., Hadiatullah, H., Schnelle-Kreis, J., Xu, Y., Yue, M., Zhang, X., Querol, X., Cao, X., Bendl, J., Cyrys, J., 2022. Levels and Drivers of Urban Black Carbon and Health Risk Assessment during Pre-and COVID19 Lockdown in Augsburg, Germany. Environ Pollut, 120529.

Long, C.M., Nascarella, M.A., Valberg, P.A., 2013. Carbon black vs. black carbon and other airborne materials containing elemental carbon: physical and chemical distinctions. Environ. Pollut. 181, 271–286.

Lu, Q., Liu, C., Zhao, D., Zeng, C., Li, J., Lu, C., Wang, J., Zhu, B., 2020. Atmospheric heating rate due to black carbon aerosols: uncertainties and impact factors. Atmos. Res. 240, 104891.

Ma, J., Tang, J., Li, S.M., Jacobson, M.Z., 2003. Size distributions of ionic aerosols measured at Waliguan Observatory: implication for nitrate gas-to-particle transfer processes in the free troposphere. J. Geophys. Res. Atmos. 108.

Markowicz, K.M., Ritter, C., Lisok, J., Makuch, P., Stachlewska, I.S., Cappelletti, D., Mazzola, M., Chilinski, M.T., 2017. Vertical variability of aerosol single-scattering albedo and equivalent black carbon concentration based on in-situ and remote sensing techniques during the iAREA campaigns in Ny-Ålesund. Atmos. Environ. 164, 431–447.

Molnar, A., Imre, K., Ferenczi, Z., Kiss, G., Gelencser, A., 2020. Aerosol hygroscopicity: hygroscopic growth proxy based on visibility for low-cost PM monitoring. Atmos. Res. 236, 104815.
Olson, M.R., Victoria Garcia, M., Robinson, M.A., Van Rooy, P., Dietenberger, M.A., Bergin, M., Schauer, J.J., 2015. Investigation of black and brown carbon multiple-wavelength-dependent light absorption from biomass and fossilfuel combustion source emissions. J. Geophys. Res. Atmos. 13, 6682–6697.
Paasonen, P., Asmi, A., Petäjä, T., Kajos, M.K., Äijälä, M., Junninen, H., Holst, T., Abbatt, J.P., Arneth, A., Birmili, W., 2013. Warming-induced increase in aerosol number concentration likely to moderate climate change. Nat. Geosci. 6, 438–442.
Pani, S.K., Wang, S., Lin, N., Chantara, S., Lee, C., Thepnuan, D., 2020. Black carbon over an urban atmosphere in northern peninsular Southeast Asia: characteristics, source apportionment, and associated health risks. Environ. Pollut. 259, 113871.
Peng, Z., Zhao, H., Lyu, H., Wang, L., Huang, H., Nan, Q., Tang, J., 2018. UV modification of biochar for enhanced hexavalent chromium removal from aqueous solution. Environ. Sci. Pollut. Res. Int. 25, 10808–10819.
Peng, J., Hu, M., Shang, D., Wu, Z., Du, Z., Tan, T., Wang, Y., Zhang, F., Zhang, R., 2021. Explosive secondary aerosol formation during severe haze in the North China Plain. Environ. Sci. Technol. 55, 2189–2207.
Petzold, A., Ogren, J.A., Fiebig, M., Laj, P., Li, S.M., Baltensperger, U., Holzer-Popp, T., Kinne, S., Pappalardo, G., Sugimoto, N., Wehrli, C., Wiedensohler, A., Zhang, X.Y., 2013. Recommendations for reporting "black carbon" measurements. Atmos. Chem. Phys. 13, 8365–8379.
Pöschl, U., 2005. Atmospheric aerosols: composition, transformation, climate and health effects. Angew. Chem. Int. Ed. 44, 7520–7540.
Rigler, M., Drinovec, L., Lavrič, G., Vlachou, A., Prévôt, A.S., Jaffrezo, J.L., Stavroulas, I., Sciare, J., Burger, J., Kranjc, I., 2020. The new instrument using a TC–BC (total carbon–black carbon) method for the online measurement of carbonaceous aerosols. Atmos. Meas. Tech. 13, 4333–4351.
Sandradewi, J., Prévôt, A.S.H., Weingartner, E., Schmidhauser, R., Gysel, M., Baltensperger, U., 2008. A study of wood burning and traffic aerosols in an Alpine valley using a multi-wavelength Aethalometer. Atmos. Environ. 42, 101–112.
Savadkoohi, M., Pandolfi, M., Reche, C., Niemi, J.V., Mooibroek, D., Titos, G., Green, D. C., Tremper, A.H., Hueglin, C., Liakakou, E., 2023. The variability of mass concentrations and source apportionment analysis of equivalent black carbon across urban Europe. Environ. Int. 178, 108081.
Schauer, J.J., Kleeman, M.J., Cass, G.R., Simoneit, B.R., 2001. Measurement of emissions from air pollution sources. 3. C1− C29 organic compounds from fireplace combustion of wood. Environ. Sci. Technol. 35, 1716–1728.
Schauer, J.J., Kleeman, M.J., Cass, G.R., Simoneit, B.R., 2002a. Measurement of emissions from air pollution sources. 4. C1− C27 organic compounds from cooking with seed oils. Environ. Sci. Technol. 36, 567–575.
Schauer, J.J., Kleeman, M.J., Cass, G.R., Simoneit, B.R., 2002b. Measurement of emissions from air pollution sources. 5. C1− C32 organic compounds from gasoline-powered motor vehicles. Environ. Sci. Technol. 36, 1169–1180.
Srivastava, P., Naja, M., 2021. Characteristics of carbonaceous aerosols derived from long-term high-resolution measurements at a high-altitude site in the central Himalayas: radiative forcing estimates and role of meteorology and biomass burning. Environ. Sci. Pollut. Res. Int. 28, 14654–14670.
Srivastava, A.K., Bisht, D.S., Ram, K., Tiwari, S., Srivastava, M.K., 2014. Characterization of carbonaceous aerosols over Delhi in Ganga basin: seasonal variability and possible sources. Environ. Sci. Pollut. Res. Int. 21, 8610–8619.
Srivastava, D., Favez, O., Petit, J., Zhang, Y., Sofowote, U.M., Hopke, P.K., Bonnaire, N., Perraudin, E., Gros, V., Villenave, E., 2019. Speciation of organic fractions does matter for aerosol source apportionment. Part 3: combining off-line and on-line measurements. Sci. Total Environ. 690, 944–955.
T Veld, M., Alastuey, A., Pandolfi, M., Amato, F., Perez, N., Reche, C., Via, M., Minguillon, M.C., Escudero, M., Querol, X., 2021. Compositional changes of PM2. 5 in NE Spain during 2009–2018: a trend analysis of the chemical composition and source apportionment. Sci. Total Environ. 795, 148728.
Trechera, P., Garcia-Marlès, M., Liu, X., Reche, C., Pérez, N., Savadkoohi, M., Beddows, D., Salma, I., Vörösmarty, M., Casans, A., 2023. Phenomenology of ultrafine particle concentrations and size distribution across urban Europe. Environ. Int. 172, 107744.
Turpin, B.J., Lim, H., 2001. Species contributions to PM2. 5 mass concentrations: revisiting common assumptions for estimating organic mass. Aerosol Sci. Technol. 35, 602–610.
van der Zee, S.C., Fischer, P.H., Hoek, G., 2016. Air pollution in perspective: health risks of air pollution expressed in equivalent numbers of passively smoked cigarettes. Environ. Res. 148, 475–483.
Verma, S., Ghosh, S., Boucher, O., Wang, R., Menut, L., 2022. Black carbon health impacts in the Indo-Gangetic plain: exposures, risks, and mitigation. Sci. Adv. 8, o4093.
Wang, Q., Jiang, N., Yin, S., Li, X., Yu, F., Guo, Y., Zhang, R., 2017. Carbonaceous species in PM2. 5 and PM10 in urban area of Zhengzhou in China: seasonal variations and source apportionment. Atmos. Res. 191, 1–11.
Wu, C., Yu, J.Z., 2016. Determination of primary combustion source organic carbon-to-elemental carbon (OC/EC) ratio using ambient OC and EC measurements: secondary OC-EC correlation minimization method. Atmos. Chem. Phys. 16, 5453–5465.
Wu, J., Lu, J., Min, X., Zhang, Z., 2018. Distribution and health risks of aerosol black carbon in a representative city of the Qinghai-Tibet Plateau. Environ. Sci. Pollut. Res. Int. 25, 19403–19412.
Xiao, W., Fu, Y., Wang, T., Lv, X., 2018. Effects of land use transitions due to underground coal mining on ecosystem services in high groundwater table areas: a case study in the Yanzhou coalfield. Land Use Pol. 71, 213–221.
Xie, Y., Liu, Z., Wen, T., Huang, X., Liu, J., Tang, G., Yang, Y., Li, X., Shen, R., Hu, B., 2019. Characteristics of chemical composition and seasonal variations of PM2. 5 in Shijiazhuang, China: impact of primary emissions and secondary formation. Sci. Total Environ. 677, 215–229.
Xu, Z., Wen, T., Li, X., Wang, J., Wang, Y., 2015. Characteristics of carbonaceous aerosols in Beijing based on two–year observation. Atmos. Pollut. Res. 6, 202–208.
Xu, J., Wang, Q., Deng, C., McNeill, V.F., Fankhauser, A., Wang, F., Zheng, X., Shen, J., Huang, K., Zhuang, G., 2018. Insights into the characteristics and sources of primary and secondary organic carbon: high time resolution observation in urban Shanghai. Environ. Pollut. 233, 1177–1187.
Yang, S., Pu, F., Wang, Z., Liu, Z., Li, M., 2022. Number concentration and size distribution of soot aerosols of heptane fire at low pressures. Fire Mater. 46, 993–999.
Yao, L., Huo, J., Wang, D., Fu, Q., Sun, W., Li, Q., Chen, J., 2020. Online measurement of carbonaceous aerosols in suburban Shanghai during winter over a three-year period: temporal variations, meteorological effects, and sources. Atmos. Environ. 226, 117408.
Yus-Díez, J., Via, M., Alastuey, A., Karanasiou, A., Minguillón, M.C., Perez, N., Querol, X., Reche, C., Ivančič, M., Rigler, M., 2022. Absorption enhancement of black carbon particles in a Mediterranean city and countryside: effect of particulate matter chemistry, ageing and trend analysis. Atmos. Chem. Phys. 22, 8439–8456.
Zhang, Y., Min, S., Zhang, Y., Zeng, L., He, L., Bin, Z., Wei, Y., Zhu, X., 2007. Source profiles of particulate organic matters emitted from cereal straw burnings. J. Environ. Sci. (China) 19, 167–175.
Zhang, H., Cheng, S., Li, J., Yao, S., Wang, X., 2019. Investigating the aerosol mass and chemical components characteristics and feedback effects on the meteorological factors in the Beijing-Tianjin-Hebei region, China. Environ. Pollut. 244, 495–502.
Zhang, Q., Sarkar, S., Wang, X., Zhang, J., Mao, J., Yang, L., Shi, Y., Jia, S., 2019. Evaluation of factors influencing secondary organic carbon (SOC) estimation by CO and EC tracer methods. Sci. Total Environ. 686, 915–930.
Zhao, P., Dong, F., Yang, Y., He, D., Zhao, X., Zhang, W., Yao, Q., Liu, H., 2013. Characteristics of carbonaceous aerosol in the region of Beijing, Tianjin, and Hebei, China. Atmos. Environ. 71, 389–398.